Bright source of polarization-entangled photons using a PPKTP pumped by a broadband multi-mode diode laser

Youn-Chang Jeong, Kang-Hee Hong, and Yoon-Ho Kim*

Department of Physics, POSTECH, Pohang, 37673, South Korea

*yoonho72@gmail.com

Abstract: We report a bright source of polarization-entangled photon pairs using spontaneous parametric down-conversion (SPDC) in a 10 mm long type-II PPKTP crystal pumped by a broadband multi-mode diode laser with the coherence length of 330 μm. Ordinarily, the huge mismatch between the pump coherence length and the PPKTP length would degrade the polarization entanglement completely. By employing the universal Bell-state synthesizer scheme, we remove the spectral/temporal distinguishability of the biphoton amplitudes entirely to recover high-visibility and high-fidelity two-photon polarization entanglement. The pair detection rates are 7,000 pairs/mW via single-mode fibers (with 99.2% fidelity) and 90,900 pairs/mW via multi-mode fibers (with 96.8% fidelity). We also analyze the scheme theoretically to show the effect of broadband multi-mode pumping on the phase matching condition of the type-II PPKTP.

OCIS codes: (270.0270) Quantum optics; (190.4410) Nonlinear optics, parametric processes.

References and links

1. K. Liao, H. Yan, J. He, S. Du, Z.-M. Zhang, and S.-L. Zhu, "Subnatural-linewidth polarization-entangled photon pairs with controllable temporal with controllable temporal length," Phys. Rev. Lett. **112**, 243602 (2014).
2. G. Juska, V. Dimastrodonato, L.O. Mereni, A. Gocalinska, and E. Pelucchi, "Towards quantum-dot arrays of entangled photon emitters," Nat. Photon. **7**, 527 (2013).
3. M. Muller, S. Bounouar, K.D. Jons, M. Glassl, and P. Michler, "On-demand generation of indistinguishable polarization-entangled photon pairs," Nat. Photon. **8**, 224 (2014).
4. Y.H. Shih and C.O. Alley, "New type of Einstein-Podolsky-Rosen-Bohm experiment using pairs of light quanta produced by optical parametric down conversion," Phys. Rev. Lett. **61**, 2921–2924 (1988).
5. P.G. Kwiat, K. Mattle, H. Weinfurter, and A. Zeilinger, A.V. Sergienko, and Y. Shih, "New high-intensity source of polarization-entangled photon pairs," Phys. Rev. Lett. **75**, 4337–4341 (1995).
6. S. Barz, G. Cronenberg, A. Zeilinger, and P. Walther, "Heralded generation of entangled photon pairs," Nat. Photon. **4**, 553–556 (2010).
7. F. Kaiser, A. Issautier, L.A. Ngah, O. Danila, H. Herrmann, W. Sohler, A. Martin, and S. Tanzilli, "High-quality polarization entanglement state preparation and manipulation in standard telecommunication channels," New J. Phys. **14** 085015 (2012).
8. P.G. Kwiat, E. Waks, A.G. White, I. Appelbaum, and P.H. Eberhard, "Ultrabright source of polarization-entangled photons," Phys. Rev. A **60**, R773–R776 (1999).
9. R. Rangarajan, M. Goggin, and P. Kwiat, "Optimizing type-I polarization-entangled photons," Opt. Express **17**, 18920–18933 (2009).
10. M. Pelton, P. Marsden, D. Ljunggren, M. Tengner, A. Karlsson, A. Fragemann, C. Canalias, F. Laurell, "Bright, single-spatial-mode source of frequency non-degenerate, polarization-entangled photon pairs using periodically poled KTP," Opt. Express **12**, 3573–3580 (2004).
11. P. Trojek and H. Weinfurter, "Collinear source of polarization-entangled photon pairs at nondegenerate wavelengths," Appl. Phys. Lett. **92**, 211103 (2008).

#254572 Received 25 Nov 2015; revised 25 Dec 2015; accepted 26 Dec 2015; published 13 Jan 2016

12. F. Steinlechner, P. Trojek, M. Jofre, H. Weier, D. Perez, T. Jennewein, R. Ursin, J. Rarity, M.W. Mitchell, J.P. Torres, H. Weinfurter, and V. Pruneri, "A high-brightness source of polarization-entangled photons optimized for applications in free space," Opt. Express **20**, 9640–9649 (2012).
13. S. Takeuchi, "Beamlike twin-photon generation by use of type II parametric downconversion," Opt. Lett. **26**, 843–845 (2001).
14. Y.-H. Kim, "Quantum interference with beamlike type-II spontaneous parametric down-conversion," Phys. Rev. A **68**, 013804 (2003).
15. X.-L. Niu, Y.-F. Huang, G.-Y. Xiang, G.-C. Guo, and Z.Y. Ou, "Beamlike high-brightness source of polarization-entangled photon pairs," Opt. Lett. **33**, 968–970 (2008).
16. H.-P. Lo, A. Yabushita, C.-W. Luo, P. Chen, and T. Kobayashi, "Beamlike photon-pair generation for two-photon interference and polarization entanglement," Phys. Rev. A **83**, 022313 (2011).
17. M. Fiorentino, C.E. Kuklewicz, and F.N.C. Wong, "Source of polarization entanglement in a single periodically poled KTiOPO4 crystal with overlapping emission cones," Opt. Express **13**, 127–135 (2005).
18. F. Steinlechner, S. Ramelow, M. Jofre, M. Gilaberte, T. Jennewein, J.P. Torres, M.W. Mitchell, and V. Pruneri, "Phase-stable source of polarization-entangled photons in a linear double-pass configuration," Opt. Express **21**, 11943–19951 (2013).
19. T.E. Keller and M.H. Rubin, "Theory of two-photon entanglement for spontaneous parametric down-conversion driven by a narrow pump pulse," Phys. Rev. A **56**, 1534–1541 (1997).
20. W.P. Grice and I.A. Walmsley, "Spectral information and distinguishability in type-II down-conversion with a broadband pump," Phys. Rev. A **56**, 1627–1634 (1997).
21. Y.-H. Kim, S.P. Kulik, M.H. Rubin, and Y. Shih, "Comment on "Dispersion-independent high-visibility quantum interference in ultrafast parametric down-conversion," Phys. Rev. Lett. **86**, 4710 (2001).
22. Y.-H. Kim, V. Berardi, M.V. Chekhova, and Y. Shih, "Anticorrelation effect in femtosecond-pulse pumped type-II spontaneous parametric down-conversion," Phys. Rev. A **64**, 011801(R) (2001).
23. A.V. Sergienko, M. Atature, Z. Walton, G. Zjaeger, B.E.A. Saleh, and M.C. Teich, "Quantum cryptography using femtosecond-pulsed parametric down-conversion," Phys. Rev. A **60**, R2622 (1999).
24. Y.-H. Kim, M.V. Chekova, S.P. Kulick, M.H. Rubin, and Y. Shih, "Interferometric Bell-state preparation using femtosecond-pulse-pumped spontaneous parametric down-conversion," Phys. Rev. A **63**, 062301 (2001).
25. M. Fiorentino and R.G. Beausoleil, "Compact sources of polarization-entangled photons," Opt. Express **16**, 20149–20156 (2008).
26. P.G. Evans, R.S. Bennink, W.P. Grice, and T.S. Humble, "Bright source of spectrally uncorrelated polarization-entangled photons with nearly single-mode emission," Phys. Rev. Lett. **105**, 253601 (2010).
27. Y.-H. Kim, S.P. Kulik, and Y. Shih, "High-intensity pulsed source of space-time and polarization double-entangled photon pairs," Phys. Rev. A **62**, 011802(R) (2000).
28. Y.-H. Kim, S.P. Kulik, and Y. Shih, "Bell-state preparation using pulsed nondegenerate two-photon entanglement," Phys. Rev. A **63**, 060301(R) (2001).
29. T.Sh. Iskhakov, I.N. Agafonov, M.V. Chekhova, and G. Leuchs, "Polarization-entangled light pulses of 10^5 photons," Phys. Rev. Lett. **109**, 150502 (2012).
30. Y.-H. Kim and W.P. Grice, "Generation of pulsed polarization-entangled two-photon state via temporal and spectral engineering," J. Mod. Opt. **49**, 2309–2323 (2002).
31. Y.-H. Kim, S.P. Kulik, M.V. Chekhova, W.P. Grice, and Y. Shih, "Experimental entanglement concentration and universal Bell-state synthesizer," Phys. Rev. A **67**, 010301(R) (2003).
32. M. Fiorentino, G. Messin, C.E. Kuklewicz, F.N.C. Wong, and J.H. Shapiro, "Generation of ultrabright tunable polarization entanglement without spatial, spectral, or temporal constraints," Phys. Rev. A **69**, 041801(R) (2004).
33. T. Kim, M. Fiorentino, and F.N.C. Wong, "Phase-stable source of polarization-entangled photons using a polarization Sagnac interferometer," Phys. Rev. A **73**, 012316 (2006).
34. A. Fedrizzi, T. Herbst, A. Poppe, T. Jennewein, and A. Zeilinger, "A wavelength-tunable fiber-coupled source of narrowband entangled photons," Opt. Express **15**, 15377–15386 (2007).
35. O. Kuzucu and F.N.C. Wong, "Pulsed Sagnac source of narrow-band polarization-entangled photons," Phys. Rev. A **77**, 032314 (2008).
36. M. Hentschel, H. Hübel, A. Poppe, and A. Zeilinger, "Three-color Sagnac source of polarization-entangled photon pairs," Opt. Express **17**, 23153–23159 (2009).
37. A. Predojevic, S. Grabher, and G. Weihs, "Pulsed Sagnac source of polarization entangled photon pairs," Opt. Express **20**, 25022–25029 (2012).
38. S.-Y. Baek, O. Kwon, and Y.-H. Kim, "High-Resolution Mode-Spacing Measurement of the Blue-Violet Diode Laser Using Interference of Felds Created with Time Delays Greater than the Coherence Time," Jpn. J. Appl. Phys. **46**, 7720–7723 (2007).
39. O. Kwon, Y.-S. Ra, and Y.-H. Kim, "Coherence properties of spontaneous parametric down-conversion pumped by a multi-mode cw diode laser," Opt. Express **17**, 13059–13069 (2009).
40. O. Kwon, K.-K. Park, Y.-S. Ra, Y.-S. Kim, and Y.-H. Kim, "Time-bin entangled photon pairs from spontaneous parametric down-conversion pumped by a cw multi-mode diode laser," Opt. Express **21**, 25492–25500 (2013).
41. A. V. Sergienko, Y. Shih, and M. H. Rubin, "Experimental evaluation of a two-photon wave packet in type-II

#254572 Received 25 Nov 2015; revised 25 Dec 2015; accepted 26 Dec 2015; published 13 Jan 2016

parametric downconversion," J. Opt. Soc. Am. B **12**, 859 (1996).
42. Y.-H. Kim, "Measurement of one-photon and two-photon wave packets in spontaneous parametric downconversion," J. Opt. Soc. Am. B **20**, 1959 (2003).
43. O. Kwon, Y.-S. Ra, and Y.-H. Kim, "Observing photonic de Broglie waves without the maximally-path-entangled $|N,0\rangle + |0,N\rangle$ state," Phys. Rev. A **81**, 063801 (2010).

1. Introduction

A source of polarization-entangled photons is an essential resource in various quantum information applications, including quantum computing, quantum teleportation, and quantum communication. Although solid state and atomic systems have recently shown the feasibility of entangled photon generation [1–3], spontaneous parametric down-conversion (SPDC) in a nonlinear optical crystal is by far the most versatile source of entangled photons due to comparably high generation rates and wide varieties of photonic quantum states SPDC can generate with high purity and fidelity.

SPDC generates photon pairs that are entangled in their spectral (and time) degrees of freedom and the degree of spectral/temporal entanglement depends on a variety of factors, including the bandwidth and coherence of the pump laser, the crystal properties, and wavelengths and polarizations of the photons. Various schemes based on SPDC have been proposed and implemented to generate polarization-entangled photon pairs. The first scheme made use of non-collinear type-I SPDC pumped by a monochromatic continuous-wave (cw) laser and a non-polarizing beam splitter for quantum interference of the photon pairs [4]. The schemes for generating polarization entangled photon pairs based on the monochromatic cw laser pumped SPDC include non-collinear type-II SPDC [5, 6], collinear type-II SPDC [7], two non-collinear type-I SPDC [8, 9], two collinear type-I SPDC [10–12], beamlike type-II SPDC [13–16], overlapping type-II emission cones [17], linear double pass scheme [18], etc.

It is important to mention that, to generate polarization-entangled photon pairs in the schemes mentioned above, the pump coherence length should be sufficiently larger than the crystal length. This requirement imposed a significant difficulty in generating polarization-entangled photons with high-purity and high-flux when the pump is switched to ultrafast lasers as the pulsed source of entangled photons have become essential for multi-photon based quantum information experiments. When type-II SPDC is pumped by an ultrafast pump with a short coherence time ($\approx$ 100 fs), the biphoton wavepackets responsible for polarization-entanglement become spectrally and temporally distinguishable, causing detrimental reduction of quantum interference [19–22]. This has forced experimentalists to use a very thin SPDC crystal and to use a narrowband spectral filters for SPDC photons to generate polarization-entangled photons, significantly reducing the useful photon flux [23].

The development of high-intensity pulsed source of polarization-entangled photons started with the somewhat unstable Mach-Zehnder scheme [24–26] and led to the interferometrically stable (but more difficult to achieve a high fidelity Bell state) cascaded crystal scheme [27–29]. In 2003, Kim *et al.* proposed and demonstrated the "universal Bell-state synthesizer" scheme in which a high-fidelity Bell state can be achieved by quantum interference of pulsed type-II SPDC at a polarizing beam splitter [30, 31]. The scheme is interferometrically stable and a high-fidelity Bell state can be achieved without spectral filtering and temporal compensation. The Sagnac scheme developed later operates on the same principle but the Bell state fidelity is affected by the quality of the dual-wavelength optics (waveplates, mirrors, and beam splitters) and the location of the nonlinear crystal within the loop [32–37] .

Experiments mentioned hitherto involved a monochromatic cw or an ultrafast pulse laser, which are bulky and expensive. Recently, high-power blue-violate cw diode lasers have become readily available at a very low cost but they have very short coherence lengths (several hundred

#254572 Received 25 Nov 2015; revised 25 Dec 2015; accepted 26 Dec 2015; published 13 Jan 2016

μm) due to the multi-mode broadband nature [38]. Coherence properties of SPDC pumped by a broadband cw multi-mode diode laser were studied [39] and it was recently reported that time-bin entangled photon pairs can be generated by broadband multi-mode pumped SPDC [40]. It is, however, a challenging problem to develop a bright source of polarization entangled photon pairs based on SPDC pumped by a broadband multi-mode diode laser. To develop a high-flux source, the use of a long periodically poled nonlinear crystal is essential. Since the pump has an extremely short coherence length on the order of several hundred μm while the length of the periodically poled nonlinear crystal is on the order of several cm, the biphoton wavepackets responsible for polarization entanglement become distinguishable, causing severe degradation of polarization entanglement [19, 20, 24]

In this paper, we report a bright source of polarization-entangled photon pairs using a 10 mm long type-II PPKTP pumped by a broadband multi-mode cw diode laser with the coherence length of 330 μm. Ordinarily, the huge mismatch between the pump coherence length and the PPKTP length would cause spectral/temporal distinguishability of the biphoton amplitudes, making it impossible to extract polarization entanglement. In this work, we adopt the "universal Bell-state synthesizer" scheme [31] and show that high-fidelity Bell-states can be generated even with such a huge mismatch between the pump coherence length and the crystal length. We demonstrate a bright source of polarization entangled photon pairs at 812 nm with the detection rate of 7,000 pairs/mW (via single-mode fibers and with the Bell-state fidelity of 99.2%) and 90,900 pairs/mW (via multi-mode fibers and with the Bell-state fidelity of 96.8%). We also demonstrate the spectral/temporal properties of the SPDC photons in a two-photon quantum interference experiment. Unlike typical type-II SPDC where the biphoton interference shows a triangular dip pattern for cw pumping and a Gaussian pattern for ultrafast pumping [31, 41, 42], the SPDC photons from the type-II PPKTP crystal exhibit the two-photon interference pattern similar to that of type-I SPDC [42]. We provide a full theoretical and numerical analysis to show that this interesting behavior is due to the interplay between the broadband cw multi-mode pumping and the phase matching condition of the type-II PPKTP.

2. Experimental setup

The schematic of the experiment is shown in Fig. 1. For generating the SPDC photons, a 10 mm long type-II PPKTP crystal with the poling period of 10 μm was used. The PPKTP crystal was pumped by a multi-mode cw diode laser operating at 406.2 nm with the full width at half maximum (FWHM) bandwidth of roughly 0.5 nm. The spatial mode of the pump laser beam was cleaned up by passing the beam through a 1 m long single-mode optical fiber (SM400, Thorlabs). The pump laser was then focused at the PPKTP crystal and the measured pump power at the input face of the PPKTP crystal was 2 mW.

The temperature of the PPKTP crystal was maintained at 86.8°C for degenerate non-collinear type-II SPDC, producing SPDC photons at the central wavelength of 812.4 nm with the FWHM bandwidth of 8.7 nm (e-ray) and 5.8 nm (o-ray). The SPDC photons make an angle of $\pm 1.3^\circ$ with respect to the pump propagation direction. Note that, in the non-critical phase matching as in this case, the e-ray and the o-ray rings of the type-II SPDC overlap to produce a single ring, rather than two orthogonally polarized diverging rings observed in typical critical phase matching [5, 13, 14].

The polarization state in the two path modes 1 and 2 in Fig. 1(a), right after the PPKTP crystal, is in fact a mixed state,

$$\frac{1}{2}(|H_1, V_2\rangle\langle V_2, H_1| + |V_1, H_2\rangle\langle H_2, V_1|), \tag{1}$$

where $|V\rangle$ and $|H\rangle$ refer to the vertical and horizontal polarization state of a single photon,

#254572 Received 25 Nov 2015; revised 25 Dec 2015; accepted 26 Dec 2015; published 13 Jan 2016

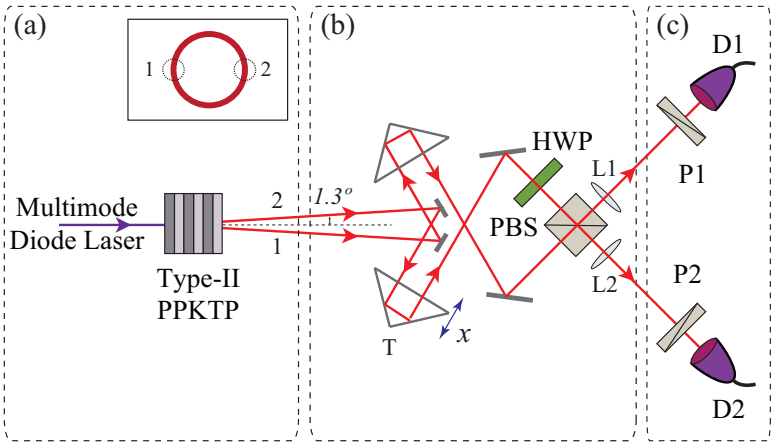

Fig. 1. Experimental schematic for the bright source of polarization-entangled photon pairs based on the "universal Bell-state synthesizer" scheme by using a 10 mm type-II PPKTP pumped by a broadband cw multi-mode diode laser. (a) Non-collinear type-II SPDC is used so that the signal (e-ray) and the idler (o-ray) photons emerge from the PPKTP crystal in overlapping concentric rings. Two conjugate path modes 1 and 2 (marked by small circles) were selected. (b) The signal and idler photons, after making their polarization state identical by using a half-wave plate (HWP), are made to overlap at the polarizing beam splitter (PBS) by a trombone prism (T) and collimated by collimation lenses (L1, L2). (c) The detection part consists of single photon detectors (D1, D2) and polarization analyzers (P1, P2).

respectively, and the subscript represents the path modes 1 and 2. This is due to the spectral/temporal distinguishability of the biphoton wavepackets introduced by the huge mismatch between the pump coherence length and the length of the PPKTP crystal [30]. The polarization mixed state is then transformed into a Bell state by using the "universal Bell-state synthesizer" scheme shown in Fig. 1(b) [31]. The SPDC photons in path modes 1 and 2 are selected and the half-wave plate (HWP) introduced in one of the input ports of the polarizing beam splitter (PBS) flips the polarization state, $|H_2\rangle \leftrightarrow |V_2\rangle$. The two photons are then overlapped at the PBS by adjusting their arrival times with a trombone prism and collimated by using collimation lenses. This scheme effectively erases the spectral/temporal distinguishability between the biphoton amplitudes $|H_1,H_2\rangle$ and $|V_1,V_2\rangle$ by re-routing e-ray and o-ray photons to the same output ports of the PBS regardless of their polarization states, so that the e-ray and the o-ray photons are always detected at D1 and D2, respectively. The photonic polarization state at the output of the PBS can then be written as a maximally entangled Bell state,

$$\frac{1}{\sqrt{2}}(|H,H\rangle + |V,V\rangle). \tag{2}$$

The polarization quantum state of the photon pair was then analyzed by two-photon quantum state tomography using a set of polarizers (P1 and P2) and single-photon detectors (D1 and D2) as shown in Fig. 1(c). No spectral filters were used before the detectors. The coincidence time window of the detectors was set at 6 ns.

#254572 Received 25 Nov 2015; revised 25 Dec 2015; accepted 26 Dec 2015; published 13 Jan 2016

3. Theoretical analysis

The density matrix ρ of the two-photon state generated via multi-mode diode laser pumped spontaneous parametric down conversion (SPDC) can be described as follows [38];

$$\rho = \int d\omega_p \mathscr{S}(\omega_p) |\psi(\omega_p)\rangle\langle\psi(\omega_p)|. \tag{3}$$

Here, $\mathscr{S}(\omega_p)$ is the spectral power density of the pump that describes the weight of each spectral mode ω_p and can be written as [39, 40, 43]

$$\mathscr{S}(\omega_p) = \frac{\sum_{n=-N}^{N} \mathscr{S}_0(\omega_p)\,\delta(\omega_p - \omega_{p0} - n\Delta\omega_p)}{\sum_{n=-N}^{N} \mathscr{S}_0(\omega_{p0} + n\Delta\omega_p)}, \tag{4}$$

where ω_{p0} is the central frequency of the pump, $\Delta\omega_p$ is the mode spacing, and n is the mode number. $\mathscr{S}_0(\omega_p)$ is the overall spectral profile of the pump that is assumed to be Gaussian centered at ω_{p0},

$$\mathscr{S}_0(\omega_p) \equiv \exp\left(-(\omega_p - \omega_{p0})^2 / \delta\omega_p{}^2\right), \tag{5}$$

with pump bandwidth $\delta\omega_p$. $|\psi(\omega_p)\rangle$ is the state of the photon pair generated via type-II non-collinear SPDC with a monochromatic pump laser of frequency ω_p and can be written as

$$\begin{aligned} |\psi(\omega_p)\rangle \sim \int dk_o dk_e \int_0^L dz e^{i\Delta z} \delta(\omega_o + \omega_e - \omega_p) \\ \times [\hat{a}_{1H}^\dagger(\omega_e)\hat{a}_{2V}^\dagger(\omega_o) + \hat{a}_{2H}^\dagger(\omega_e)\hat{a}_{1V}^\dagger(\omega_o)]|0\rangle, \end{aligned} \tag{6}$$

where $\hat{a}_{1H}^\dagger(\omega)$ and $\hat{a}_{1V}^\dagger(\omega)$, respectively, are the creation operator for a horizontally and a vertically polarized photon of frequency ω in mode 1 right after the crystal in Fig. 1. For mode 2, $\hat{a}_{2H}^\dagger(\omega)$ and $\hat{a}_{2V}^\dagger(\omega)$ are defined similarly. Δ is the phase mismatch between the pump photon and down-converted photons, and L is the length of the crystal. Note that, in the non-critical phase matching as in this case, the e-ray and the o-ray rings of the type-II SPDC overlap to produce a single ring, rather than two orthogonally polarized diverging rings observed in typical critical phase matching [5, 13, 14]. Due to the use of PPKTP in generating the SPDC photons, the phase mismatch term is given as,

$$\Delta = k_p - k_e - k_o - 2\pi/\Lambda, \tag{7}$$

where k_p, k_e, and k_o are the k-vector of pump, e-polarized and o-polarized photons within the PPKTP medium, respectively. The poling period of the crystal is Λ.

The spectral properties of type-II SPDC photon pairs can then be described by expanding the phase mismatch term Δ about the central frequencies of the pump Ω_p, e-polarized Ω_e, and o-polarized Ω_o photons. To the first order in frequency, we obtain

$$\Delta = \Delta_0 - (\omega_p - \Omega_p)D_+ - \frac{1}{2}(\omega_o - \omega_e)D, \tag{8}$$

where we set $\Omega_p = \omega_{p0}$ and

$$\Delta_0 = K_p - K_e - K_o - 2\pi/\Lambda \tag{9}$$

is the zeroth order phase mismatch term with $K_i = k_i(\Omega_i)$ with $i = p, e$ and o. Under the ideal condition $\Delta_0 = 0$ but in general this term is not zero even in the best circumstances. Other terms in eq. (8) are defined as

$$D_+ = \left[\frac{1}{u_o(\Omega_o)} + \frac{1}{u_o(\Omega_e)}\right] - \frac{1}{u_o(\Omega_p)}, \tag{10}$$

#254572 Received 25 Nov 2015; revised 25 Dec 2015; accepted 26 Dec 2015; published 13 Jan 2016

and

$$D = \frac{1}{u_o(\Omega_o)} - \frac{1}{u_e(\Omega_e)}, \tag{11}$$

where $u_o(\omega)$ and $u_e(\omega)$, respectively, are the group velocities of o-polarized and e-polarized photons inside the crystal.

The coincidence count rate at the detectors D1 and D2 can be described as

$$R_c \propto \int dt_1 dt_2 \ \mathrm{tr}\left[\rho E_1^{(-)}(t_1) E_2^{(-)}(t_2) E_2^{(+)}(t_2) E_1^{(+)}(t_1)\right], \tag{12}$$

where

$$E_1^{(+)}(t_1) = \frac{1}{\sqrt{2}} \int d\omega [\hat{a}_{1H}(\omega) + e^{i\omega\tau} \hat{a}_{2V}(\omega)] e^{-i\omega t_1} \tag{13}$$

and

$$E_2^{(+)}(t_2) = \frac{1}{\sqrt{2}} \int d\omega [\hat{a}_{1V}(\omega) \pm e^{i\omega\tau} \hat{a}_{2H}(\omega)] e^{-i\omega t_2} \tag{14}$$

are the positive frequency components of the quantized electric fields at D1 at time t_1 and D2 at time t_2 [24], respectively. Here, $\tau = x/c$ where x is the optical path length difference between the two paths in Fig. 1(b). The $\pm$ sign in $E_2^{(+)}(t_2)$ refer to the two orthogonal polarization projection basis. When the polarization analyzer P2 in front of D2 is set at $|D\rangle = \frac{1}{\sqrt{2}}(|H\rangle + |V\rangle)$, the $+$ sign should be chosen and, when P2 is set at $|A\rangle = \frac{1}{\sqrt{2}}(|H\rangle - |V\rangle)$, the $-$ sign is chosen. Evaluating the above equation leads to the coincidence count rate,

$$R_c = 1 \pm \mathscr{T}(\tau), \tag{15}$$

where the $\pm$ sign represents the two-photon polarization projection basis for P1 and P2: $+$ for $(|D\rangle, |D\rangle)$ and $-$ for $(|D\rangle, |A\rangle)$. The term $\mathscr{T}(\tau)$ responsible for two-photon quantum interference is given as

$$\mathscr{T}(\tau) = \int d\omega_p \mathscr{S}(\omega_p) \cos\left[\left\{\frac{2D_+}{D}(\omega_{p0} - \omega_p) + \frac{2\Delta_0}{D}\right\}\tau\right] \mathrm{tri}\left(\frac{2}{\pi L D}\tau\right). \tag{16}$$

Here, the triangular function is defined by

$$\mathrm{tri}\,(x) = \max\,(1-x, 0)\,, \tag{17}$$

where $\max\,(a,b)$ yields the largest of a and b.

4. Experimental results

First, we study the biphoton interference as a function of path length difference τ. The polarization analyzers P1 and P2 are set at two orthogonal serttings ($|D\rangle$, $|D\rangle$) and ($|D\rangle$, $|A\rangle$). The interferometric path length difference τ are then scanned to observe spectral/temporal properties of the biphoton states involved in the two-photon interference. The experimental results are shown in Fig. 2. In Fig. 2(a), we show the experimental data when single-mode fiber coupled detectors are used. The interference visibility calculated from the data is 0.978. When multimode fiber coupled detectors are used, the visibility slightly dropped to 0.936 but more than ninefold increase in the two-fold count rate is observed, see Fig. 2(b).

It is noteworthy to mention that the SPDC photons from type-II PPKTP pumped by a broadband multi-mode cw diode laser exhibit rather unique biphoton interference structure. It has

#254572 Received 25 Nov 2015; revised 25 Dec 2015; accepted 26 Dec 2015; published 13 Jan 2016

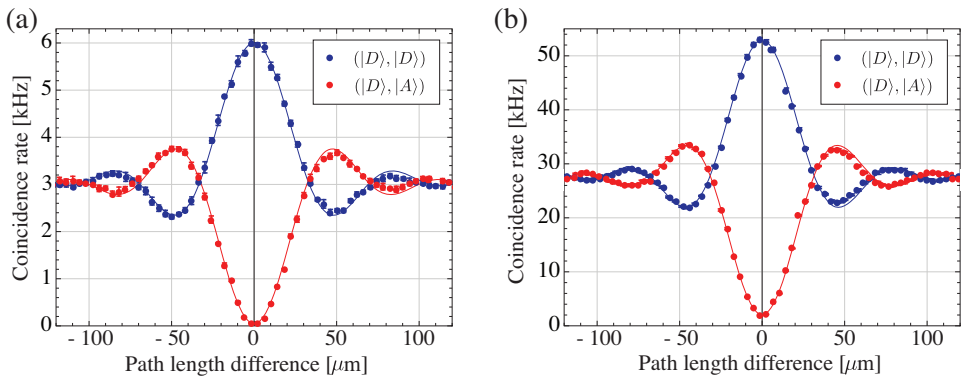

Fig. 2. Experimental data showing high-visibility two-photon quantum interference when (a) single-mode fiber coupled detectors are used and (b) multi-mode fiber coupled detectors are used. The inset shows the settings of the polarization analyzers P1 and P2. The visibilities are 0.978 for (a) and 0.936 for (b). The solid lines are curves due to Eq. (15), obtained by summing up the effect of 50 most dominant modes of multi-mode diode laser with 0.015nm mode spacing. The best fitting is obtained when the PPKTP temperature is set at 79.6°C although the measured temperature is 86.8°C. This discrepancy is due to systematic errors in the temperature measurement (as the location of the thermocouple in our setup was a bit far from the PPKTP crystal).

long been known that monochromatic cw laser pumped type-II SPDC photons exhibit triangular biphoton interference shape [31, 41, 42]. For mode-locked ultrafast laser pumped type-II SPDC, the biphoton interference shape is rather close to a Gaussian [31]. In the case of broadband multi-mode cw laser pumped type-II SPDC as in this case, the biphoton interference shown in Fig. 2 exhibits damped oscillatory behaviors which resemble monochromatic cw pumped type-I SPDC [42].

This hitherto unobserved effects can be explained by carefully studying Eq. (16), which shows the effect of group velocity differences of the pump and SPDC photons to the overall shape of the two-photon interference. Equation (16) contains two terms, one responsible for the triangular biphoton interference shape and the other responsible for sinusoidal oscillation, both as functions of the path length difference τ. As the triangular term is rather well known [31, 41, 42], we focus on the cosine term in Eq. (16) which includes the effect of the 0th order phase mismatch Δ_0 and the broadband multi-mode nature of the cw pump laser. When τ is varied, the biphoton interference is modulated due to the coefficient $\frac{2D_+}{D}(\omega_{p0}-\omega_p)+\frac{2\Delta_0}{D}$ which shows the effect of a particular frequency mode of the pump. As Eq. (16) contains summation over all frequency modes in the pump and, for each frequency mode, the modulation period is slightly different, the net result is the damped oscillatory behavior of the two-photon interference as shown in Fig. 2. Note that the function $\mathrm{tri}\left(\frac{2}{\pi LD}\tau\right)$, which would give the triangular shape, turns out to be much larger in width than the damped oscillatory shape due to the fact that, in our case,

$$\frac{2D_+}{D}(\omega_{p0}-\omega_p)+\frac{2\Delta_0}{D} \gg \frac{2}{\pi LD}. \tag{18}$$

This is the complete opposite case of the monochromatic cw pumped type-II SPDC where only the triangular shape two-photon interference structure appears. That is, the argument of the cosine term in Eq. (16) becomes zero for the monochromatic cw pumped type-II SPDC.

We now consider the quality of Bell states generated using this scheme. To generate the Bell state, we set the path length difference $\tau = 0$ and we reconstruct the density matrix of

#254572 Received 25 Nov 2015; revised 25 Dec 2015; accepted 26 Dec 2015; published 13 Jan 2016

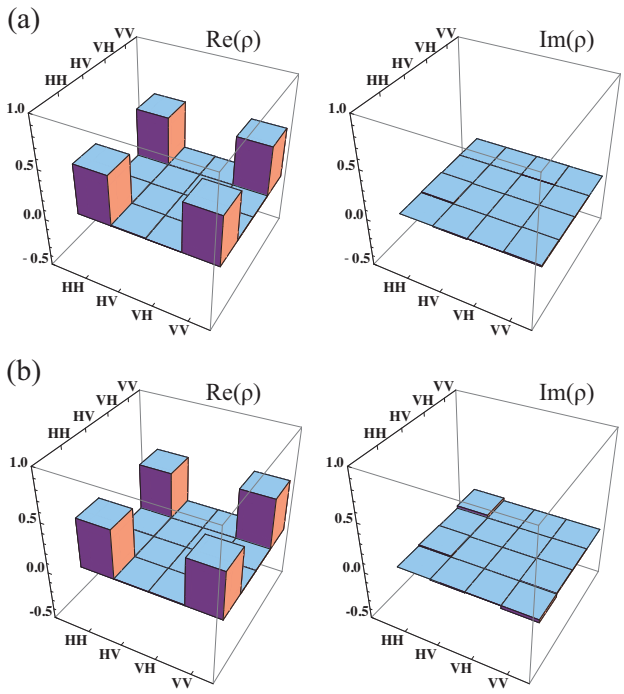

Fig. 3. The reconstructed density matrix of the generated Bell state. The entangled state with respect to $\frac{1}{\sqrt{2}}(|H,H\rangle + |V,V\rangle)$ has fidelity 0.992 and 0.968 for photon pairs coupled into (a) single-mode fibers and (b) multi-mode fibers for detection. Concurrence, which quantifies the amount of two-qubit entanglement, is for (a) 0.983 and for (b) 0.937.

the two-photon polarization state by using quantum state tomography. The results are shown in Fig. 3. As shown in Fig. 3, high fidelity Bell states are generated. Concurrence $\mathscr{C}$, which quantifies the amount of two-qubit entanglement, is calculated from the reconstructed density matrix: $\mathscr{C} = 0.983$ for Fig. 3(a) and $\mathscr{C} = 0.937$ for Fig. 3(b).

The experimental results demonstrate an ultra-bright and high-fidelity source of polarization-entangled photon pair by using the universal Bell state synthesizer scheme. By using commercial Si-SPAD (Perkin Elmer SPDC-AQR) with the quantum efficiency of $\sim$50% at 810 nm, we achieved the coincidence count rate of 7,000 pair$\cdot$mW^{-1} for single-mode fiber coupling and 90,900 pair$\cdot$mW^{-1} for multi-mode fiber coupling.

There indeed has been a remarkable progress in achieving a high-flux source of polarization entangled photon pairs in recent years. To put our work into context, it is worth looking at a few notable results in high-flux sources of entangled photon pairs. Steinlechner *et al.* has demonstrated coincidence detection rates of 16 kHz (by using two 20 mm long type-0 PPKTP and at 25 μW pump power) [12] and 11.8 kHz (by using a 11 mm long type-0 PPKTP and at 10.4 μW pump power) [18]. Here, however, the pump coherence length must be greater than the crystal length to achieve high fidelity Bell states. The Sagnac scheme is more versatile and the coincidence detection rate of 82 kHz (by using a 25 mm long type-II PPKTP and at 1 mW pump power) has been achieved [34]. This approach however requires high quality dual-wavelength optics for high fidelity Bell states. In our work, by adopting the Bell state synthesizer scheme, we have shown that it is possible to achieve a stable, high flux, and high fidelity source of Bell states albeit using a low cost diode pump laser and off-the-shelf optics.

#254572 Received 25 Nov 2015; revised 25 Dec 2015; accepted 26 Dec 2015; published 13 Jan 2016

5. Conclusion

By using a low-cost diode laser emitting a broadband multimode cw laser beam with a short coherence length (330 μm) and a 10 mm long type-II PPKTP crystal, we built a bright source of Bell states. In the usual type-II SPDC, it is not possible to erase the temporal and spectral distinguishabilities completely when the mismatch between the pump coherence length and the length of the nonlinear crystal is big. We have adopted the universal Bell-state synthesizer scheme to remove the spectral/temporal distinguishabilities completely, hence building a high fidelity and high brightness source of Bell states. We have achieved the polarization entangled photon pairs at 812 nm with the pair detection rate of 7,000 pairs/mW (via single-mode fibers) and 90,900 pairs/mW (via multi-mode fibers). We have also demonstrated an unusual two-photon interference experiment. Unlike typical type-II SPDC where the biphoton interference shows a triangular dip pattern for cw pumping and a Gaussian pattern for ultrafast pumping, the SPDC photons from the type-II PPKTP crystal exhibit the two-photon interference pattern similar to that of type-I SPDC. We have provided a full theoretical and numerical analysis to show that this interesting behavior is due to the interplay between the broadband cw multi-mode pumping and the phase matching condition of the type-II PPKTP.

Acknowledgments

This work was supported in part by the National Research Foundation of Korea (Grant No. 2013R1A2A1A01006029).

#254572 Received 25 Nov 2015; revised 25 Dec 2015; accepted 26 Dec 2015; published 13 Jan 2016